Evaluation of Entire Ovine Cartilage Repair Articular Surfaces: Mechanical and Electromechanical Assessment

S. Sim[1,2], I. Hadjab[1,2], M. Garon[2], E. Quenneville[2],
M.B. Hurtig[3], M.D. Buschmann[1,4], and C.D. Hoemann[1,4]

1. Institute of Biomedical Engineering, Polytechnique Montreal, Montreal, Quebec, Canada 2. Biomomentum Inc., Laval, Quebec, Canada 3. Comparative Orthopaedic Research Laboratory, Department of Clinical Studies, University of Guelph, Guelph, Ontario, Canada. 4. Department of Chemical Engineering, Polytechnique Montreal, Montreal, Quebec, Canada

KEYWORDS: Cartilage Repair, Indentation, Electromechanics

Purpose: *To demonstrate the ability of non-destructive electromechanical device and automated indentation technique in assessing the quality of cartilage in a sheep model of cartilage repair.* ***Methods:*** *Ex vivo electromechanical and mechanical mappings of articular surfaces (~40 positions/map) were performed over distal condyles from 5 treated sheep (8 – 9 y-o, 9 months post-surgery, bone marrow stimulation model) and 2 control sheep (8 y-o). Electromechanical measurements were performed manually with the Arthro-BST (Biomomentum, Laval) which calculates a quantitative parameter (QP) (in A.U.) based on compression-induced streaming potentials measured by 37 microelectrodes lying on a semi-spherical indenter (d=6.4mm). Mechanical assessments (structural stiffness) were conducted at the same positions using an automated indentation technique with a multiaxial tester (Mach-1 v500css, Biomomentum, Laval) equipped with a spherical indenter (d=1mm). Selected sites were additionally analyzed by histology and by unconfined mechanical compression tests.* ***Results:*** *GAG-rich repair tissues displayed poroelastic mechanical behavior. According to electromechanical and mechanical properties mappings on control and treated articular surfaces, some para-defect articular surfaces showed lower average structural stiffness and weaker electromechanical properties (high QP) vs matching control regions. The QP was lower and structural stiffness higher in the repair site. Repair site soft tissue thickness varied from 0 to 1200 µm (mean thickness 315±260 µm, n=10) compared to ~1100 µm in flanking areas. Surface GAG depletion was observed at the defect border in some of the repaired medial condyles.* ***Conclusion:*** *Mechanical measures demonstrated poroelastic cartilage behavior in repair tissues of aged sheep. Measurements outside the repair sites are suggestive of modest cartilage GAG depletion and consistent with previous data (Hoemann et al., 2005; Custers et al., 2009). As for the repair site, the increase in the structural stiffness and decrease in the QP could be partly due to repair cartilage thickness being lower than normal cartilage thickness. This study indicates the utility of functional mapping techniques in large animal cartilage repair studies.*

Purpose: There are currently no suitable alternatives for histology in evaluating the quality of cartilage repair tissue (Hoemann et al., 2011). Our group has been focusing on new, non-destructive methods to evaluate cartilage repair through its electromechanical and mechanical properties. These quantitative measurements could reveal crucial information needed to discriminate hyaline from fibrocartilagenous tissues. While mechanical properties have always been a reliable indicator of the functional properties of cartilage (Armstrong & Mow, 1982), electromechanical properties also provide functional assessment information of cartilage that relates to structure and composition (Sim et al., 2014). In the current study, electromechanical properties of repair cartilage at 9 months post-operative in an aged sheep model of marrow stimulation were measured with a hand-held medical device, the Arthro-BST. Mechanical properties were measured with a novel automated indentation mapping technique using the Mach-1. Biopsies were also taken and analyzed by traditional unconfined mechanical compression and by histology in sections at the test sites. The purpose of this study was to demonstrate the ability of rapid and non-destructive mapping techniques (Arthro-BST and automated indentation) to assess functional properties of repair cartilage and its integration to the surrounding articular surface in a sheep model.

Material & Methods: All procedures involving animals were carried out according to institutionally-approved protocols. Five mature sheep (8-9 year old) underwent bone marrow stimulation by microdrilling 11 holes (1.4 mm burr diameter) in a 10x10mm full-thickness cartilage defect created in the medial condyle of both knees. In one knee, drill holes were further treated by a freeze-dried chitosan scaffold. Sheep were sacrificed 9 months post-surgery. In addition, two mature sheep (8 year old) having no surgical intervention served as controls (intact). The distal condyles from the right and left stiffle joints of the treated and control sheep were harvested with a band saw, so that the lateral and medial condyles remained together in one piece.

The distal condyles were secured in a sample holder and placed in a testing chamber filled with phosphate-buffered saline (PBS, Sigma, St. Louis, MO, USA). A camera-registration system (Mapping Toolbox, Biomomentum, Laval) was used to obtain a top

view image of the distal condyles and to superimpose a position grid (~40 positions) to allow electromechanical and mechanical testing of the same sites over the entire articular surface.

Electromechanical *ex vivo* mappings of those articular surfaces were first performed using the Arthro-BST. This hand-held medical device has a semi-spherical indenter (effective diameter = 6.4 mm, microelectrode density = 5.1 electrodes/mm^2) which measures the electromechanical properties of cartilage under load through a quantitative parameter (QP) corresponding to the number of microelectrodes on the spherical indenter in contact with the cartilage when the sum of their streaming potential reaches 100 mV. Thus, the electromechanical QP is inversely proportional to the electromechanical activity of cartilage, i.e. cartilage with lower glycosaminoglycan levels or weaker collagen structure will have QPs higher than the control. The lateral and medial condyles of each sample were electromechanically mapped in about 30 minutes. The QP data were interpolated to a rainbow colormap using the Mapping Toolbox software, where brown/red is high QP and blue is low QP.

Mechanical *ex vivo* mappings were subsequently performed using an automated indentation technique with the Mach-1 v500css on which a spherical indenter (d=1mm) was attached under its multiaxial load cell (z-resolution: 100 nm & 350 mg). This automated indentation technique detects the perpendicular direction at each position and moves a spherical indenter along this direction (indentation amplitude of 200 μm at 200 μm/s) while measuring the normal component of the resulting force. The structural stiffness (load (N) divided by the indentation depth (mm)) was calculated at each position. Altered cartilage could have a lower or higher structural stiffness compared to matching locations in the control. Each treated condyle was mechanically mapped in about 30 minutes. The structural stiffness obtained at 50 μm indentation depth was interpolated to a rainbow colormap using Mapping Toolbox software, where brown/red is high structural stiffness and blue is low structural stiffness.

Jamshidi needles (11G) were then used to extract one osteochondral core at the repair site of each treated condyle for unconfined compression mechanical testing with the Mach-1 tester (10% strain precompression followed by five 2% compression stress relaxations stopped when relaxation rate reached 0.05N/min). Another biopsy was collected by shaving a small area of repair cartilage in the distal defect for biochemical analyses. Load *vs*. displacement curves were fit to the fibril-reinforced poroelastic model (Soulhat et al., 1999) to obtain the fibril modulus (E_f), equilibrium modulus (E_m), and permeability (k) (assuming Poisson's ratio of 0).

Distal condyles were fixed in 10% neutral buffered formalin for histological analysis. Each sample was decalcified in 0.5N HCl/0.1% glutaraldehyde, cut in the sagittal plane into 3 blocks, and 5 µm paraffin sections generated in the test point areas, using calibrated line measures in digital images of the histology samples, and a RM2155 (Leica) motorized microtome. The sections were stained with Safranin O-Fast Green and calibrated digital scans generated at 40x magnification (Hamamatsu Photonics, Hamamatsu, Japan). The slides were then associated with the position grid where the electromechanical and mechanical properties were obtained. Histomorphometry measures were carried out by 2 blinded readers using Northern Eclipse (Empix, Mississauga, ON, Canada) to make line measures of minimal thickness and maximal thickness for 3 evenly spaced sagittal sections in the repair tissue area covering the drill holes. The collective mean and standard deviation of the minimal and maximal tissue thickness for all condyles is reported (n=10).

Statistical analysis were performed on the mean of each region (I, II, III, IV and V defined in Fig. 1) for each treated sheep (n=10) and each control sheep (n=4). An unequal variance t-test was then performed in order to examine the difference between structural stiffness and electromechanical QP of treated and control for each region. All statistical analyses were performed with SAS version 9.3 (SAS Institute Inc., Cary, North Carolina, USA).

Results:

Electromechanical and Mechanical Mapping

Electromechanical and mechanical (indentation) cartilage properties were compared between repaired condyles and age-matched intact condyles (control), in the 5 regions. Needle penetration tests were performed to measure cartilage thickness of intact condyles but not in repaired condyles. In general, in control articular surfaces, thicker cartilage showed lower structural stiffness and higher QP values (Fig. 1). A similar mean stiffness and QP were seen in control (n=4) and surgical groups (n=10) in the unoperated LFC (test regions I & II) and distal condyle near the intercondylar notch (test region III). By contrast, repair cartilage tissues (test region V) showed a significantly higher mean stiffness and lower mean electromechanical QP compared to matching regions of intact knees, whereas the outer rim of the distal condyle (test region IV) had a slight but significantly lower stiffness and higher electromechanical QP in operated *vs* matching control area. The distal condyles of many operated knees (regions III and IV) had a slightly roughened macroscopic appearance below the repaired cartilage defect.

Histology and Poroelastic Behavior

GAG-rich repair tissues (hyaline-like repair) showed poroelastic mechanical behavior characterized by an increase of the stress during a ramp displacement, a rapid decrease of stress right after compression and a stress relaxation during constant compression (Fig. 2A-B). Moreover, the mechanical behavior of cartilage shown for high-quality hyaline-like repair and thinner hyaline-like repair displays a typical poroelastic behavior where the peak stress is approximately two or three times higher than the equilibrium stress. However, when the test site consists of unrepaired subchondral bone or calcified cartilage, poroelastic behavior was not evident due to a thin or non-existent cartilage layer, as can be seen on the corresponding histological slide (Fig. 2C). Indeed, from bone-only to high-quality hyaline repair, the structural stiffness decreases while the electromechanical QP increases with the quality of the repair. Also, histological results showed a variation in the thickness of the repair site (from 0 to 1200 µm, mean thickness 315±260 µm, n=10) compared to ~1100 µm for native cartilage at the edge of the defect.

In addition, native cartilage at the edge of the defect showed surface GAG depletion in around half of the operated medial condyles (Fig.2A, C, black arrows).

Unconfined compression on cores

Hyaline cartilage is expected to have high fibril modulus, high matrix modulus and low permeability while a GAG-depleted hyaline-like cartilage or fibrous tissue should have a lower fibril and matrix modulus and a high permeability. Unconfined compression parameters for three repair tissue cores having hyaline to GAG-depleted cartilage appearance on histological slides are shown on Figure 3. Fibril modulus goes from 13.04 MPa to 0.83 MPa from hyaline to GAG-depleted while matrix modulus goes from 0.59 MPa to 0.02 MPa respectively. As for the permeability, hyaline-like repair cartilage was $0.0021x10^{12}$ $mm^4/N{\cdot}s$ whereas repair cartilage with low levels of GAG was $0.29x10^{12}$ $mm^4/N{\cdot}s$. Also, the Jamshidi biopsy site (black arrowhead) generated to perform unconfined compression tests in the repaired lesion can be seen on histological slides and will complicate histological scoring of repair tissue in these sections (Fig. 3 *vs* Fig. 2).

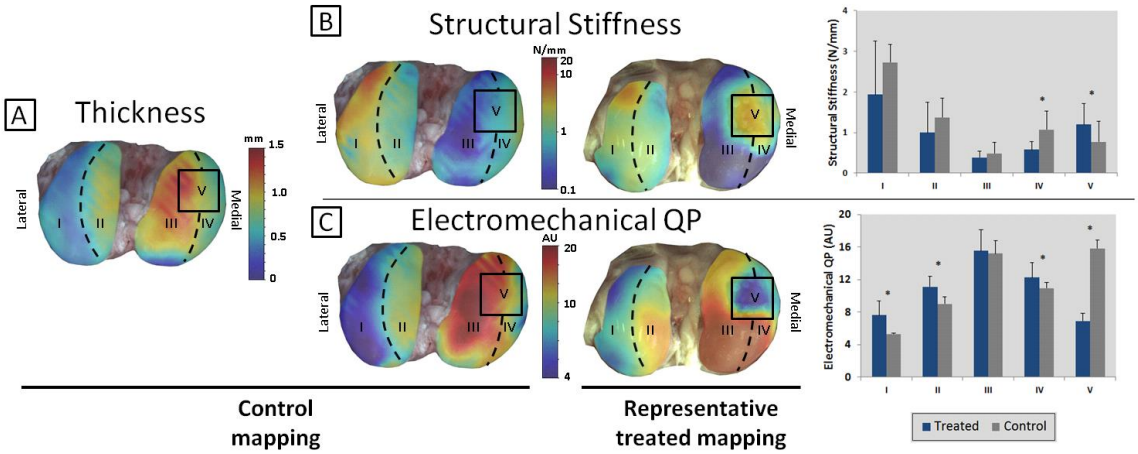

Figure 1. Average thickness, mechanical and electromechanical mappings of control samples and representative mechanical and electromechanical mappings of treated condyles. The control mapping was created by interpolating and averaging mappings from the 4 untreated femoral condyles. A) Thickness of control femoral condyles obtained through a needle technique; B) Mechanical structural stiffness at 50 µm indentation amplitude of averaged control and one representative treated femoral condyle. Bar graph of the structural stiffness at 50 µm for each regions for comparison between all control and all treated condyles; C) Electromechanical average QP mapping of control samples and one representative treated femoral

condyles. Bar graph of the electromechanical QP for each regions for comparison between all control and all treated condyles; Left joints were mirrored to represent mappings in a standardized right-hand format. Structural stiffness and electromechanical QP are presented for each region as the averaged of all control (n=4) and all treated condyles (n=10), *p<0.05.

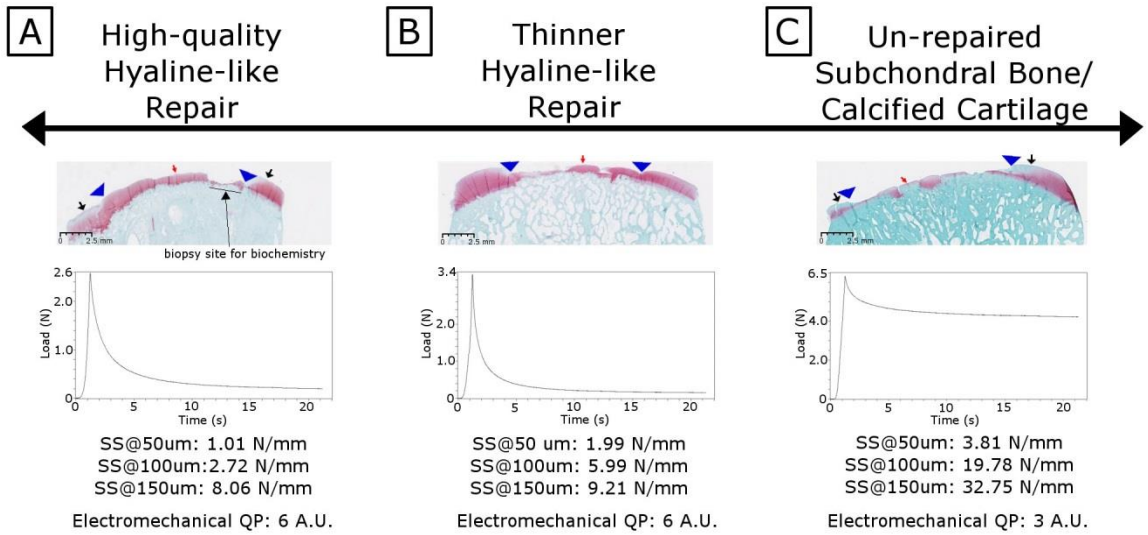

Figure 2. Representative histological slide of different cartilage repair outcomes (red arrow) with blue arrowhead delimiting the defect boundaries. A) High-quality hyaline-like repair showed poroelastic mechanical behavior; B) Thinner hyaline-like repair also showed poroelastic mechanical behavior; C) Un-repaired subchondral bone or calcified cartilage does not have a poroelastic mechanical behavior. GAG depletion is observed in regions adjacent to the repair site (black arrow). Increasing electromechanical QP and poroelastic behavior along with decreasing structural stiffness parallels increasing quality of the repair.

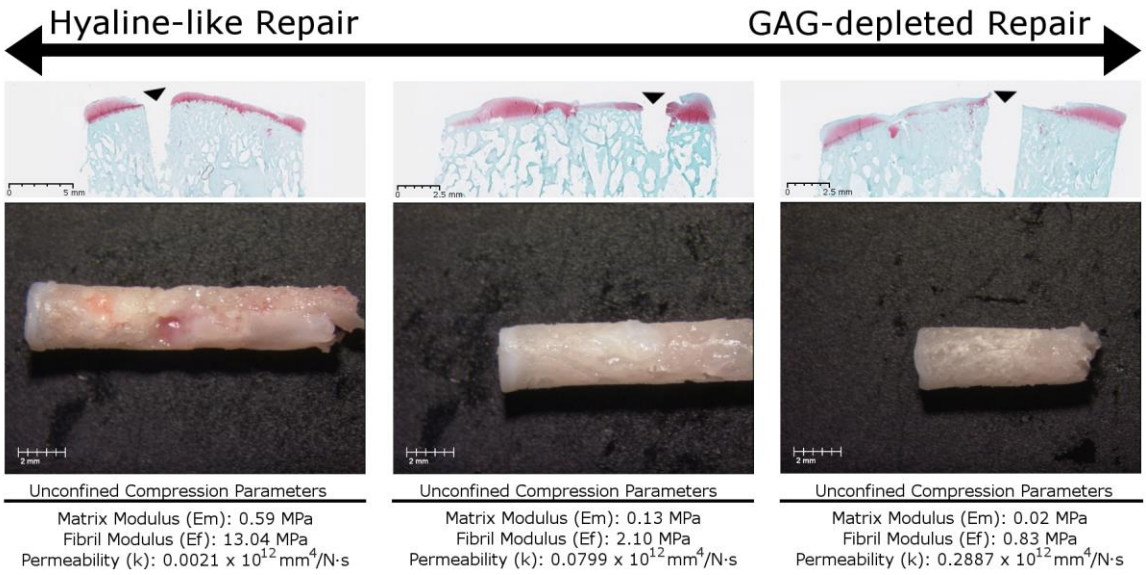

Figure 3. Biopsy sites (black arrowhead) shown in histological slides and below the corresponding macroscopic image of the biopsy and unconfined compression parameters of the non-calcified tissue on top of the biopsy. Hyaline cartilage has fibril modulus of at least 2 MPa, matrix modulus of at least 0.10 MPa and low permeability while GAG-depleted cartilage has lower fibril modulus, lower matrix modulus and higher permeability. However, in histology section, the hole resulting from the biopsy site prevents full histological scoring or histomorphometry of repair tissue area in this section.

Conclusion:

Mechanical characterisation revealed poroelastic cartilage behavior in repair tissues in aged sheep (Fig. 2). Measurements outside the repair sites are suggestive of slight surgery-induced surface cartilage degradation in the distal condyle (Fig. 1 & 2) which is consistent with previous data (Custers et al., 2009; Hoemann et al., 2005). As for the repair site, the increase in the structural stiffness could be partly explained by the thinner repair cartilage (Fig. 2). The decrease in QP in some repair tissues could be partly due to uneven resurfacing that does not permit uniform contact of all microelectrodes at the test site. Also, traditional unconfined compression parameters show higher compressive properties for hyaline repair and lower properties for fibrocartilage repair (Fig. 3), consistent with previous data (Bell et al., ICRS 2013).

Our mechanical and electromechanical measurements on age-matched and site-matched control condyles suggest that it is possible to quantitatively predict repair tissue quality of experimental condyles. The difference between the measured value and the control value

could be calculated at site-matched positions. A value close to zero thus corresponds to normal cartilage which is the aim of every cartilage repair technique, to produce a tissue that resembles native cartilage. However, few limitations needs to be considered in this study. At first, sheep in this study are aged animal model with thinner repair, the curvature diameter of the Arthro-BST indenter tip has not been optimized for the assessment of cartilage layer this thin. This limits the number of electrodes that could be in contact with the cartilage. Moreover, the irregular resurfaced defect could cause the probe to indent on a tissue tuff that is only contacting some of the electrodes. In those cases, the electromechanical QP is the same for a high-quality hyaline-like repair vs thinner hyaline-like repair (Fig. 2A vs. B). As for mechanical properties, a high structural stiffness in the repair site is explained by the fact that repair tissues in many test sites were less than 200 μm thick, suggesting that many measurements reflect resistance to compression by repair bone in addition to repair cartilage. Another limitation of this study is the over-indentation of the repair test sites, due to the decision to avoid needle thickness tests, accompanied by the unexpected thinner repair tissue in the aged animal model. Effectively, in this particular study, a constant indentation displacement (200 μm at 200 μm/s) has been used. Subsequent histology revealed that thin tissue or bone are present with a mean thickness of 315±260 μm in the repaired defects. Therefore, a constant amplitude of 200 μm could over-indent some sites. Data obtained in this study suggests that future tests using the Mach-1 automated indentation should first perform a needle penetration to measure thickness and use it so that the indentation be performed to a predefined strain level. The needle test for thickness is slightly destructive, but not as much as taking a Jamshidi biopsy core for unconfined compression tests. Histological scoring is still possible after needle tests to obtain tissue thickness. Therefore, data in this study show the potential for obtaining a useful quantitative assessment of repair tissue quality performed with intact (control) sheep cartilage, when tissue thickness is a controlled variable. Future experiments with smaller probe design aim to generate a quantitative assessment for relatively thin repair tissues compared to human tissues and irregularly resurfaced defects in animal models of cartilage repair.

It is worth mentioning that the size of the indenters used for electromechanical and mechanical assessments are different. Indeed, the indenter for mechanical assessment is smaller (d=1mm) and could indent between focal repair tissue surrounded by bone, while the indenter for electromechanical assessment is larger (d=6.4mm) reflecting the quality of tissue averaged over a larger contact area. In the future, size-matched indenters will be used to facilitate comparison between electromechanical and mechanical assessments.

In unconfined compression tests, intrinsic parameters were obtained to quantify the quality of the cartilage repair, including the fibril modulus, matrix modulus and permeability which are in accordance with previous studies in regard to the coupling of mechanical properties with histological structure (Bell et al., ICRS2013). However, the biopsy site can be seen in the corresponding histological slide (Fig. 3) which can be quite inconvenient when assessing histological score and histomorphometry in that area. Therefore, the non-destructive nature of the Arthro-BST and the novel automated indentation technique have the potential to overcome this limitation of traditional mechanical test (unconfined compression).

In summary, two novel non-destructive techniques, the Arthro-BST and the automated indentation, were applied for the first time to obtain rapidly the electromechanical and mechanical properties of entire articular surfaces in a cartilage repair study in sheep. After minor adjustments in the test protocol, these techniques have the potential to provide critical electromechanical and mechanical data about the sample without the need of taking biopsy cores that destroys its integrity and compromises further histological assesments. Moreover, these mapping techniques have demonstrate their capabilities in highlighting the spatial distribution of the parameters characterizing the repaired cartilage and its integration with the surrounding articular surface. This study has shown a relation between the electromechanical QP and indentation parameters (structural stiffness) with traditional assessments such as histology and unconfined compression in a cartilage repair study. These results demonstrate the utility of functional mapping techniques in large animal cartilage repair studies.

Acknowledgements:

This study was funded by the Canadian Institutes of Health Research (CIHR, MOP 185810, 303615), Natural Sciences and Engineering Council of Canada (CRD PJ 445265 12) and Fonds de la Recherche Quebec Santé (FRQ-S, National Researcher, CDH).The authors thank Gaoping Chen, Genevieve Picard, Jessica Guzman, and Adriana Houle for histology contributions.

References:

Armstrong, C. G., & Mow, V. C. (1982). Variations in the intrinsic mechanical properties of human articular cartilage with age, degeneration, and water content. *J Bone Joint Surg Am, 64*(1), 88-94.

Custers, R. J., Saris, D. B., Dhert, W. J., Verbout, A. J., van Rijen, M. H., Mastbergen, S. C., Creemers, L. B. (2009). Articular cartilage degeneration following the treatment of focal cartilage defects with ceramic metal implants and compared with microfracture. *J Bone Joint Surg Am, 91*(4), 900-910. doi: 10.2106/JBJS.H.00668

Hoemann, C., Kandel, R., Roberts, S., Saris, D. B. F., Creemers, L., Mainil-Varlet, P., . . . Buschmann, M. D. (2011). International Cartilage Repair Society (ICRS) Recommended Guidelines for Histological Endpoints for Cartilage Repair Studies in Animal Models and Clinical Trials. *Cartilage, 2*(2), 153-172. doi: Doi 10.1177/1947603510397535

Hoemann, C.D. , Hurtig, M, Rossomacha, E., Sun, J, Chevrier, A. , Shive, MS., & Buschmann, MD. (2005). Chitosan-glycerol phosphate/blood implants improve hyaline cartilage repair in ovine microfracture defects. *Journal of Bone and Joint Surgery-American Volume, 87A*(12), 2671-2686. doi: 10.2106/JBJS.D.02536

Sim, S., Chevrier, A., Garon, M., Quenneville, E., Yaroshinsky, A., Hoemann, C. D., & Buschmann, M. D. (2014). Non-destructive electromechanical assessment (Arthro-BST) of human articular cartilage correlates with histological scores and biomechanical properties. *Osteoarthritis Cartilage, 22*(11), 1926-1935. doi: 10.1016/j.joca.2014.08.008

Bell, A., Chen, G., Quenneville, E., Hurtig, M. B., Hoemann, C. D. (2013). Novel unconfined compression test using Jamshidi osteochondral biopsies couples biomechanical properties with histological structure. 11th World Congress of the International Cartilage Repair Society, Abstract 5712.